HHS Public Access

Author manuscript

J Invest Dermatol. Author manuscript; available in PMC 2015 December 01.

Published in final edited form as:

J Invest Dermatol. 2015 June ; 135(6): 1649–1658. doi:10.1038/jid.2014.503.

The tryptophan-derived endogenous arylhydrocarbon receptor ligand 6-formylindolo[3,2-*b*]carbazole (FICZ) is a nanomolar UVA-photosensitizer in epidermal keratinocytes

Sophia L. Park[#], **Rebecca Justiniano**[#], **Joshua D. Williams**, **Christopher M. Cabello**, **Shuxi Qiao**, and **Georg T. Wondrak**[*]

Department of Pharmacology and Toxicology, College of Pharmacy & Arizona Cancer Center, University of Arizona, Tucson, AZ, USA

[#] These authors contributed equally to this work.

Abstract

Endogenous UVA-chromophores may act as sensitizers of oxidative stress underlying cutaneous photoaging and photocarcinogenesis, but the molecular identity of non-DNA key chromophores displaying UVA-driven photodyamic activity in human skin remains largely undefined. Here we report that 6-formylindolo[3,2-b]carbazole (FICZ), a tryptophan photoproduct and endogenous high affinity aryl hydrocarbon receptor (AhR) agonist, acts as a nanomolar photosensitizer potentiating UVA-induced oxidative stress irrespective of AhR ligand activity. In human HaCaT and primary epidermal keratinocytes, photodynamic induction of apoptosis was elicited by the combined action of solar simulated UVA and FICZ, whereas exposure to the isolated action of UVA or FICZ did not impair viability. In a human epidermal tissue reconstruct, FICZ/UVA-cotreatment caused pronounced phototoxicity inducing keratinocyte cell death, and FICZ photodynamic activity was also substantiated in a murine skin exposure model. Array analysis revealed pronounced potentiation of cellular heat shock, ER stress, and oxidative stress response gene expression observed only upon FICZ/UVA-cotreatment. FICZ photosensitization caused intracellular oxidative stress, and comet analysis revealed introduction of formamidopyrimidine-DNA glycosylase (FPG)-sensitive oxidative DNA lesions suppressible by antioxidant cotreatment. Taken together, our data demonstrate that the endogenous AhR ligand FICZ displays nanomolar photodynamic activity representing a molecular mechanism of UVA-induced photooxidative stress potentially operative in human skin.

Keywords

photosensitization; UVA; FICZ; arylhydrocarbon receptor; skin photooxidative stress

[*]**Corresponding author**: Georg T. Wondrak, Ph.D., University of Arizona, College of Pharmacy and Arizona Cancer Center, 1515 North Campbell Avenue, Tucson, AZ 85724 USA; wondrak@pharmacy.arizona.edu; phone: 520-626-9009.

CONFLICT OF INTEREST

The authors state no conflict of interest.

INTRODUCTION

The causative role of ultraviolet (UV) photons in skin photoaging and photocarcinogenesis is firmly established. UVA (320 - 400 nm) radiation results in little photoexcitation of DNA directly, and cutaneous generation of reactive oxygen species (ROS) and organic free radicals is now a widely accepted mechanism of UVA-phototoxicity (Agar *et al.*, 2004; Wondrak *et al.*, 2006; Cadet *et al.*, 2009; Zastrow *et al.*, 2009; Marionnet *et al.*, 2010). In addition to various molecular sources including NAD(P)H oxidase and mitochondrial electron leakage that may contribute to cutaneous ROS formation in response to UV-exposure, skin chromophores may act as endogenous photosensitizers causing either direct substrate oxidation (type I) or activation of molecular oxygen (type II) upstream of cellular oxidative stress (Scharffetter-Kochanek *et al.*, 1997; Baier *et al.*, 2006; Wondrak *et al.*, 2006). In human skin, various chromophores have been proposed as endogenous UV-sensitizers, including protoporphyrin IX (Kennedy and Pottier, 1992), urocanic acid (Menon and Morrison, 2002), riboflavin (Sato *et al.*, 1995), B_6-vitamers (Wondrak *et al.*, 2004), melanin precursors (Kipp and Young, 1999), collagen crosslinks (Wondrak *et al.*, 2003), and advanced glycation and lipid peroxidation endproducts (Lamore *et al.*, 2010a). However, molecular identity and causative involvement of relevant endogenous skin photosensitizers remain poorly understood (Wondrak *et al.*, 2006).

In addition to a role in the generation of ROS through excitation of endogenous preexisting photosensitizers, we have recently demonstrated that acute exposure to solar UV can also cause the formation of potent photosensitzers in human skin (Williams *et al.*, 2014). Recently, the UVB-driven formation of the L-tryptophan-derived photoproduct 6-formylindolo[3,2-*b*]carbazole (FICZ) in human HaCaT keratinocytes has been demonstrated (Fritsche *et al.*, 2007). Importantly, FICZ displays activity as a high affinity arylhydrocarbon receptor (AhR) agonist more potent than TCDD (2,3,7,8 tetratchlorodibenzo-*p*-dioxin) (Wincent *et al.*, 2009), and the significance of FICZ-dependent AhR signaling in immune modulation, circadian rhythm, xenobiotic metabolism, as well as skin barrier function and photocarcinogenesis has been explored (Fritsche *et al.*, 2007; Mukai and Tischkau, 2007; Quintana *et al.*, 2008; Luecke *et al.*, 2010; Haarmann-Stemmann *et al.*, 2012; Esser *et al.*, 2013; Magiatis *et al.*, 2013; Tigges *et al.*, 2014). It is well established that FICZ upregulates expression of AhR target genes including *CYP1A1* (encoding cytochrome P450, family 1, member A1), involved in metabolic activation of carcinogenic polycyclic aromatic hydrocarbons. Indeed, the initial observation that UVB exposure can cause *CYP1A1* upregulation through AhR activation was mechanistically resolved by the identification of FICZ as an UVB-generated endogenous AhR ligand in human keratinocytes, and additional evidence for the occurrence of FICZ in human tissue has been presented (Wei *et al.*, 1999; Katiyar *et al.*, 2000; Oberg *et al.*, 2005; Fritsche *et al.*, 2007; Wincent *et al.*, 2009; Wincent *et al.*, 2012). Importantly, in addition to UVB-induced formation from tryptophan, recent research has demonstrated that FICZ is a common metabolite of Malassezia yeasts detectable in skin scale extracts from patients with Malassezia-associated diseases including seborrheic dermatitis (Magiatis *et al.*, 2013). In contrast to metabolically inert synthetic AhR ligands such as TCDD that cause sustained AhR signaling, FICZ undergoes rapid metabolic inactivation by CYP1A1, and it has been suggested that light-driven formation of this

endogenous AhR ligand followed by transient AhR signaling and rapid enzymatic turnover represent the components of a photobiological signaling cascade operative in human skin (Rannug and Fritsche, 2006; Wincent *et al.*, 2012).

In contrast to prior investigations that have examined AhR-directed activities of FICZ detected in keratinocytes and human skin (Fritsche *et al.*, 2007; Magiatis *et al.*, 2013), no research has explored the possibility that photoexcitation of this indolo[3,2-*b*]carbazole chromophore may be associated with photobiologically relevant effects that occur independent of AhR-related mechanisms. Here we present experimental evidence suggesting that FICZ displays nanomolar photodynamic activity as a photosensitizer targeting human epidermal keratinocytes and reconstructed human epidermis with pronounced potentiation of UVA-induced oxidative, proteotoxic, and genotoxic stress responses irrespective of AhR ligand activity.

RESULTS

Array analysis identifies FICZ as a sensitizer of UVA-induced stress response gene expression in human keratinocytes

First, mass spectrometric, UV-VIS, and fluorescence spectroscopic characterization of the commercial FICZ preparation used in our experiments was performed, indicating that FICZ displays pronounced absorptivity and fluorescence throughout the UVA-1 and blue visible portions of the solar spectrum (Figure 1a).

Next, it was demonstrated that FICZ treatment causes rapid and transient nuclear translocation of AhR in human HaCaT keratinocytes observable within 15 min continuous exposure (Figure 1b) together with pronounced upregulation of protein levels of CYP1A1, an established major AhR target gene (Figure 1c).

Using the Human Oxidative Stress RT^2 Profiler™ PCR Expression Array technology we then explored the possibility that FICZ treatment may modulate UVA-induced stress response gene expression (Figure 1d; supplementary Figure S1a). Array analysis compared transcriptional profiles elicited in human HaCaT keratinocytes in response to the combined or isolated exposure to FICZ (100 nM) and solar simulated UVA (6.6 J/cm^2). We observed that only in response to exposure to the combined action of FICZ and UVA, pronounced stress response gene expression was induced. Genes upregulated in response to combined FICZ/UVA treatment were indicative of induction of oxidative (e.g. *HMOX1, AKR1C2, SQSTM1, TXNRD1, GPX3*) and proteotoxic stress responses (e.g. *HSPA6, HSPA1A, DDIT3*). In contrast to stress response gene expression that was only responsive to the combined action of FICZ and UVA, pronounced upregulation of the AhR target gene *CYP1A1* was observed in all groups exposed to FICZ (FICZ only and FICZ/UVA) irrespective of UVA exposure.

FICZ causes UVA-induced oxidative stress and impairment of genomic integrity

Next, we observed the rapid induction of stress response signaling elicited in HaCaT keratinocytes by FICZ/UVA cotreatment within 1h, including dual activational phosphorylation of p38 (Thr180/Tyr182) MAPK and inhibitory phosphorylation of eIF2α

(eukaryotic translation initiation factor), established hallmarks of cell stress signaling in skin cells greatly potentiated by FICZ (Figure 2a). Likewise, upregulation of cellular NAD(P)H-quinone oxidoreductase (NQO1) and heme oxygenase I (HO-1) protein levels was also observed in response to FICZ/UVA cotreatment (Figure 2b and supplementary Figure S1b), but protein levels of thioredoxin reductase 1 (TXNRD1), upregulated at the mRNA level (Figure 1d), remained unchanged. We also observed that FICZ/UVA cotreatment impaired mitochondrial transmembrane potential (Δψ8;m), observable by JC-1 flow cytometry within 1 h (Figure 2c).

The nature of FICZ/UVA-induced cytotoxicity was further explored by assessing photodynamic induction of oxidative stress (Figure 2d-l). Flow cytometric analysis of FICZ/UVA treated cells (Figure 2d) indicated the generation of reactive species of sufficient longevity, such as protein peroxides (Wright *et al.*, 2003), capable of oxidizing the indicator dye DCFH during cell loading after irradiation, an effect suppressed if photodynamic treatment occurred in the presence of the singlet oxygen quencher NaN_3. Moreover, direct formation of superoxide anions by UVA/FICZ photosensitization was demonstrated using the chemical NBT reduction assay performed in the absence or presence of SOD (Figure 2e). UVA-driven formation of the NBT reduction product NBF occurred as a function of FICZ concentration and was suppressed when UVA exposure occurred in the presence of SOD, consistent with NBT photoreduction downstream of FICZ-sensitized formation of superoxide anions (Wondrak *et al.*, 2002).

We also observed that FICZ is a sensitizer of UVA-induced photooxidative damage targeting isolated macromolecules (peptides and plasmid DNA) as well as genomic DNA in HaCaT keratinocytes (Figure 2f-l). Sensitization of macromolecular damage by FICZ was studied examining photooxidation of melittin ($C_{131}H_{229}N_{39}O_{31}$, Mw 2845.80, monoisotopic peak), previously used as a model target in studies of peptide oxidation and radiation damage (Figure 2f) (Lamore *et al.*, 2010a). The peptide melittin remained either untreated or underwent UVA-irradiation (3.3 J/cm^2) in the presence or absence of FICZ (100 nM). MALDI-TOF mass spectrometry revealed that only UVA exposure in the presence of FICZ induced the formation of a reaction product displaying a mass increase of 32 u [2877.74 u - 2845.76 u, monoisotopic peaks] suggesting the FICZ-sensitized introduction of molecular oxygen into the target, a mass increase completely suppressed if exposure occurred in the presence of the singlet oxygen quencher NaN_3 (Lamore *et al.*, 2010a).

Next, photodynamic introduction of DNA damage was examined using a chemical plasmid cleavage assay enhanced by Fpg (formamido-pyrimidine)-endonuclease digestion visualizing sites of DNA base oxidation including 8-oxodG through enzymatic generation of strand breaks (Figure 2g-i) (Wondrak *et al.*, 2002;Lamore *et al.*, 2010b). Indeed, only the combined action of UVA and FICZ followed by Fpg-digestion was sufficient to cause the formation of nicked target DNA. Dose response analysis revealed that low nanomolar concentrations of FICZ are sufficient to induce the UVA-driven formation of Fpg-sensitive sites, and photodynamic cleavage of plasmid DNA was completely suppressed in the presence of antioxidants known to act as excited state quenchers and singlet oxygen antagonists [NaN_3, 1,4-diazabicyclo[2.2.2]octane (DABCO), L-histidine].

Genotoxic consequences of FICZ/UVA exposure were also observed in HaCaT keratinocytes employing the comet assay enhanced by Fpg-digestion performed at various time points after treatment (0-6 h; Figure 2j-l). Consistent with photodynamic introduction of oxidized DNA base lesions, HaCaT keratinocytes exposed to the combined (but not the isolated) action of FICZ and UVA followed by Fpg-digestion displayed a NaN_3-suppressible increase in comet tail moment. A statistically significant increase in comet tail moment was already detectable when analysis was performed immediately after exposure ('0 h') and increased further over an extended incubation period ('6 h'), an observation consistent with the known amplification of photo-oxidative damage by subsequent free radical chain reactions downstream of initial oxidative insult.

FICZ is a nanomolar photosensitizer of UVA-induced keratinocyte cell death

Photodynamic induction of skin cell death by FICZ/UVA co-treatment was examined by morphological analysis (transmission electron and light microscopy; Figure 3a) and flow cytometric analysis of annexinV/PI-stained cells performed 24 h after treatment (Figure 3b). We observed that viability of HaCaT keratinocytes exposed to the combined action of high concentrations of FICZ (100 nM) and UVA (6.6 J/cm^2) was completely abolished. Consistent with the induction of apoptosis, FICZ/UVA-induced cell death was associated with caspase 3 activation (Figure 3c) and could be suppressed by cotreatment using zVADfmk, a potent pan-caspase inhibitor (Figure 3d). Moreover, cell viability was preserved if photodynamic treatment occurred in the presence of the singlet oxygen quencher NaN_3 (10 mM; Figure 3d), and FICZ photodynamic activity was enhanced by depletion of the cellular antioxidant glutathione employing the glutathione biosynthesis inhibitor buthionine sulfoximine (BSO, 1 mM, 24 h pretreatment; Figure 3e), findings that suggest an oxidative mechanism underlying FICZ phototoxicity.

Next, the dose response relationship underlying FICZ sensitization of UVA-induced cell death was explored indicating that FICZ concentrations as low as 5 nM and small doses of UVA ($\geq$ 0.33 J/cm^2) were sufficient to cause pronounced photodynamic effects (Figure 3f-g). In contrast, UVA-preirradiation of FICZ followed by incubation of un-irradiated cells using pre-irradiated FICZ did not mimic the effects of FICZ/UVA co-exposure suggesting that photodynamic induction of HaCaT cell death depends on the formation of a short-lived cytotoxic factor (such as singlet oxygen or other ROS) that is absent from the pre-irradiated FICZ preparation (Figure 3f; 'pre'). Remarkably, UVA-driven photodynamic activity of FICZ surpassed that of established endogenous photosensitizers including protoporphyrin IX (PPIX) and riboflavin (vitamin B_2) that were active only in the upper nano- (100 nM) or lower micromolar (10 μM) range, respectively (Figure 3f).

Next, based on absorbance in the blue light region we employed a monochromatic visible photoexcitation source (460 nm, LED) in order to assess feasibility of achieving visible light-driven FICZ-dependent photodynamic effects (Figure 3h). Indeed, FICZ displayed pronounced blue light-driven photodynamic activity that was antagonized by either NaN_3-cotreatment or pre-incubation using zVADfmk, observations matching the blockade of FICZ/UVA-induced cell death as detected above (Figure 3d).

The deformylated FICZ-derivative indolo[3,2-b]carbazole (ICZ) does not display photodynamic activity

In order to explore the structure activity relationship of FICZ-induced photodynamic effects we also examined the FICZ-derivative indolo[3,2-b]carbazole (ICZ), a close structural analogue and potent AhR agonist devoid of the carbaldehyde function contained in FICZ (supplementary Figure S2a) (Wincent *et al.*, 2009). Consistent with the established AhR ligand activity of ICZ, we observed ICZ-induced upregulation of *CYP1A1* expression at the protein and mRNA level irrespective of UVA exposure (supplementary Figure S2c and g). In contrast, ICZ was devoid of any UVA-driven photodynamic activity as indicated by morphological inspection (transmission electron and light microscopy; supplementary Figure S2b), flow cytometric analysis of viability (supplementary Figure S2d) and oxidative stress induction (supplementary Figure S2e). Likewise, in response to exposure to the combined action of ICZ and UVA stress response gene expression remained unchanged at the mRNA and protein levels (NQO1 and HO-1; supplementary Figure S2f and g).

Photodynamic activity of FICZ can be observed in dermal fibroblasts, primary human epidermal keratinocytes, and an organotypic epidermal skin reconstruct

UVA-induced photodynamic activity of low nanomolar concentrations of FICZ was also observed when human dermal Hs27 fibroblasts were exposed to the combined action of FICZ and UVA (6.6 J/cm^2) (Figure 4a), accompanied by changes at the mRNA level indicative of stress response gene expression (*HMOX1, DDIT3, HSPA6*; Figure 4b). In accordance with earlier reports that document constitutive attenuation of AhR signaling in dermal fibroblasts, we observed that FICZ exposure (FICZ only or FICZ/UVA combination) failed to upregulate *CYP1A1* mRNA levels indicating again that FICZ photodynamic effects occur in the absence of AhR-mediated signaling.

Next, photodynamic effects of FICZ were confirmed in primary human epidermal keratinocytes (HEKs; Figure 4c and d) and reconstructed human epidermis undergoing short term culture in growth medium supplemented with FICZ (Figure 4e). One day after UVA exposure, only the tissue reconstructs that had received FICZ/UVA combination treatment displayed pronounced phototoxicity as evident from detection of pycnotic/eosinophilic features and caspase 3-positivity, changes consistent with photodynamic induction of cell death that affected 100 % of keratinocytes situated in the basal layer of the epidermis. Photodynamic effects of FICZ were also observed in an acute exposure model in murine skin (Figure 4f). When SKH-1 mice received FICZ topical treatment followed by UVA exposure, photodynamic induction of pronounced epidermal necrosis together with Hsp70 upregulation were observed, molecular changes that were not detected in skin exposed to the isolated action of either topical FICZ or UVA. Moreover, as early as 48h after FICZ-UVA photodynamic treatment signs of regenerative reepithelialization and tissue remodeling originating from the hair follicles were observable.

DISCUSSION

UVA-sensitization by specific cutaneous chromophores is an important mechanism of skin cell photooxidative stress that contributes to photoaging and carcinogenesis (Wondrak *et al.*,

2006). Here we demonstrate that the L-tryptophan-derived photoproduct and AhR ligand FICZ displays nanomolar UVA-driven photodynamic activity as substantiated by (*i*) photooxidation of isolated macromolecules (Figure 2f-i), (*ii*) photooxidative stress and cytotoxicity in cultured human skin cells (Figure 2a-d and j-l; Figure 3; Figure 4a-d), and (*iii*) tissue damage observable in human reconstructed epidermis (Figure 4e) as well as murine skin (Figure 4f).

Remarkably, FICZ photosensitization is observable in the low nanomolar concentration range suggesting that FICZ exhibits extraordinary photodynamic potency (Figure 3f). Comparative sensitization experiments demonstrated that the UVA-induced photodynamic potency of FICZ surpasses that of established endogenous photosensitizers including riboflavin and protoporphyrin IX, an observation that to the best of our knowledge supports the conclusion that FICZ is the most potent endogenous UVA photosensitizer identified as of today. We also observed that FICZ photodynamic activity could be elicited by either UVA or blue light photoexcitation, a finding consistent with its UV/VIS absorption characteristics (Figure 1a).

Prior investigations have demonstrated the UV-driven photochemical transformation of L-tryptophan leading to the formation of specific photoproducts, some of which display activity as endogenous photosensitizers, such as N-formylkynurenine known to be a micromolar sensitizer of photooxidative stress during aging of the human lens (Andley and Clark, 1989). However, in spite of an extensive body of evidence that explores the emerging role of the tryptophan photoproduct FICZ in AhR-dependent modulation of skin barrier function and photocarcinogenesis, no research has focused on the direct photochemical and photobiological reactivities of this UVA/VIS chromophore. FICZ photodynamic potency surpasses that of other tryptophan-derived micromolar sensitizers including N-formyl-kynurenine and xanthurenic acid by more than one thousand fold, but the specific mechanistic involvement of FICZ versus other tryptophan-derived metabolites and photoproducts in mediating skin photooxidative stress remains to be elucidated. In this context, it should be emphasized that independent of its solar UV-driven origin FICZ has now been identified as a common metabolite of commensal *Malassezia* yeasts involved in the causation of cutaneous inflammatory pathologies such as seborrheic dermatitis, and detailed LC-MS analysis has demonstrated unambiguously that a microbiome-derived pool of FICZ (and other tryptophan-metabolites with unexplored phototoxicity) exists constitutively in human skin (Magiatis *et al.*, 2013).

Importantly, photodynamic activity of FICZ observed by us in skin cells and tissue does not depend on AhR signaling, as supported by the fact that (*i*) FICZ photoreactivity associated with ROS formation and substrate oxidation can be observed in cell-free chemical systems, (*ii*) FICZ-induced stress response signaling, introduction of photooxidative DNA damage, and loss of mitochondrial transmembrane potential can be observed within minutes of FICZ/UVA exposure, and (*iii*) FICZ-sensitized UVA-photodamage occurs in fibroblasts displaying strongly attenuated or absent AhR signaling. Finally, (*iv*) the deformylated FICZ-derivative ICZ, an established AhR agonist of comparable potency, was completely devoid of UVA-driven photodynamic activity (supplementary Figure S2). The differential photodynamic activity of FICZ and ICZ suggests that it is the excited state chemistry

associated with the carbaldehyde moiety (attached to the common indolocarbazole UVA-chromophore) that allows efficient intersystem crossing and triplet state formation underlying phototoxicity, a reactivity documented with numerous carbonyl-group containing UVA-photosensitizers such as benzophenone-related chromophores. However, the complex UVA-driven photochemistry of FICZ that may involve the combined mode of type I and type II photosensitization awaits further photochemical investigations.

In summary, our experimental data suggest that two molecular pathways may operate simultaneously mediating FICZ-dependent effects in human skin downstream of its formation as a cutaneous microbial metabolite or solar UVB-induced tryptophan photooxidation product (supplementary Figure S3). First, as demonstrated earlier, FICZ may modulate skin cell function through an AhR-dependent pathway (Fritsche *et al.*, 2007; Magiatis *et al.*, 2013), a mechanism that may contribute to inflammatory dysregulation and carcinogenesis as suggested before (Agostinis *et al.*, 2007; Gaitanis *et al.*, 2012; Esser *et al.*, 2013; Tigges *et al.*, 2014). In addition, as demonstrated in this prototype study, photoexcitation of FICZ by solar UVA (and potentially visible) photons causes photodynamic effects leading to the induction of cutaneous oxidative stress that may potentially exacerbate AhR-dependent cutaneous pathologies. However, it remains to be shown that in human skin, exposed to full spectrum solar UV, initial UVB-driven formation of the AhR agonist FICZ from tryptophan is followed by UVA-dependent photosensitization reactions, an emerging mechanism of skin phototoxicity that integrates photosensitizer generation driven by one spectral fraction of solar UV (UVB) with photosensitizer activation driven by another fraction (UVA). Future experimentation will aim at examining the occurrence of UV-driven versus microbial FICZ formation and its mechanistic involvement in AhR-dependent and -independent human skin photobiology.

MATERIALS AND METHODS

Chemicals

6-Formylindolo[3,2-*b*]carbazole (FICZ; CAS#:172922-91-7) was purchased from Enzo, Inc. (Plymouth Meeting, PA). Indolo[3,2-*b*]carbazole (ICZ; CAS#: 6336-32-9) was purchased from Tractus (Perrineville, NJ). All other chemicals were from Sigma (St. Louis, MO).

Spectroscopy and mass spectrometry

Mass spectrometric analysis and UV-VIS/fluorescence spectroscopy were performed as described in ‘Supplementary Materials and Methods’ online (Lamore *et al.*, 2010a).

Irradiation with solar simulated UVA and blue light

Irradiation with solar simulated UVA and blue light occurred as described in ‘Supplementary Materials and Methods’ online (Wondrak *et al.*, 2003; Lamore *et al.*, 2010a).

Cell culture

Dermal neonatal foreskin Hs27 fibroblasts from ATCC and human immortalized HaCaT keratinocytes were cultured in DMEM containing 10% fetal bovine serum (Wondrak *et al.*,

2008). Primary human epidermal keratinocytes [adult HEKa (C-005-5C)] were cultured on collagen matrix protein coated dishes using Epilife medium (EDGS growth supplement; Life Technologies, Carlsbad, CA).

Human epidermal skin reconstructs

EpiDerm™ tissues (EPI-200, 9 mm diameter, 6-well format; MatTek, Ashland, MA) were treated with FICZ [100 nM final concentration in 0.9 ml EPI-200-ASY media per well], followed by culture at 37 °C for 6 h. Before irradiation, inserts were rinsed with PBS and then UVA-exposed. After irradiation, tissue inserts were cultured for another 24 h in media. Tissue was then processed for paraffin embedment followed by H&E staining and immunohistochemical analysis.

Immunocytochemical detection of AhR nuclear translocation

For immunocytochemistry, cells were pelleted by centrifugation and processed for paraffin embedding. For AhR detection (sc-5579, Santa Cruz Biotechnology), staining was performed using a streptavidin biotin peroxidase system with a phosphatase substrate and a hematoxylin counter stain.

Human Oxidative Stress RT^{2}Profiler™ PCR Expression array analysis

Preparation of total cellular RNA, reverse transcription, and Human Oxidative Stress RT^{2}Profiler™ PCR Expression Array (SuperArray) profiling were performed as described in ‘Supplementary Materials and Methods’ online (Lamore *et al.*, 2010b; Qiao *et al.*, 2013).

Detection of intracellular oxidative stress

Induction of intracellular oxidative stress by photosensitization was analyzed by flow cytometry using 2′,7′-dichlorodihydrofluorescein diacetate (DCFH-DA) as a non-fluorescent precursor dye following a published standard procedure (Wondrak *et al.*, 2004; Lamore *et al.*, 2010c).

Mitochondrial transmembrane potential

Mitochondrial transmembrane potential ($\Delta\psi m$) was assessed using the potentiometric dye 5,5′,6,6′-tetrachloro-1,1′,3,3′-tetraethylbenzimidazolyl-carbocyanine iodide (JC-1; Sigma, T4069) following our published procedure (Qiao *et al.*, 2013).

Immunoblot analysis

Immunoblot analysis was performed following our published standard procedures. The following primary antibodies were used: CYP1A1 (sc-20772, Santa Cruz Biotechnology), total p38 (#9212, Cell Signaling, Danvers, MA), phospho-p38 (#9211, Cell Signaling), total eIF2α (#9722, Cell Signaling), phospho-eIF2α (#9721, Cell Signaling), HO-1 (#5853, Cell Signaling). Use of HRP-conjugated goat anti-rabbit (111-035-144) or goat anti-mouse secondary antibody (115-035-146, Jackson Immunological Research) was followed by visualization using enhanced chemiluminescence detection reagents.

Plasmid Cleavage Assay

DNA strand breakage was measured by the conversion of supercoiled ΦX-174 RF1 double-stranded DNA (SC-DNA) (New England Biolabs) to open circular form (OC) as described elsewhere (Wondrak *et al.*, 2002).

Comet assay (alkaline single cell gel electrophoresis)

The alkaline Comet assay was performed according to the manufacturer's instructions (Trevigen, Gaithersburg, MD, USA) as described in 'Supplementary Materials and Methods' online (Wondrak *et al.*, 2003; Lamore *et al.*, 2010b).

Transmission Electron Microscopy (TEM)

Specimens were examined using a CM12 transmission electron microscope (FEI) operated at 80 kV with digital image collection as described recently (Qiao *et al.*, 2013).

Flow cytometric analysis of cell viability

Induction of cell death was confirmed by annexin-V-FITC/propidium iodide (PI) dual staining of cells using an apoptosis detection kit according to the manufacturer's specifications (APO-AF, Sigma, St. Louis, MO).

Caspase-3 activation assay

Treatment-induced caspase-3 activation was examined using a cleaved/activated caspase-3 (asp 175) antibody (Alexa Fluor 488 conjugate, Cell Signaling, Danvers, MA, USA) followed by flow cytometric analysis as published recently (Lamore *et al.*, 2010a).

Superoxide assay

Chemical formation of superoxide radical anions during FICZ photosensitization was determined using the photometric NBT reduction assay, confirmed by scavenging of superoxide using superoxide dismutase (SOD) as detailed in 'Supplementary Materials and Methods' online (Wondrak *et al.*, 2002).

Mouse skin photodynamic treatment using FICZ

SKH-1 hairless female mice (Charles River Laboratories) were maintained under 12-h light/dark cycles receiving water and food *ad libitum*. At the beginning of the experiment, 8-week old mice (n=12) were divided into 4 groups (n=3): (1) control (DMSO only), (2) UVA + DMSO, (3) FICZ in DMSO, (4) UVA + FICZ in DMSO. Solar simulated UVA dose was 6.6 J/cm^2. 'FICZ' (in DMSO; 1 mM final concentration) or 'DMSO only' were applied topically to dorsal skin areas (20 μl total volume). After 10 min, UVA or mock irradiation were performed. Mice were maintained for another 48 h and then sacrificed. Dorsal skin was harvested and processed for (histo)-pathological examination and further IHC analysis (Hsp70). Animal experimental procedures and protocol have been reviewed and approved by the University of Arizona Institutional Animal Care and Use Committee (PHS Assurance No. A-3248-01; #11-316).

Hematoxylin and eosin (H&E) staining and immunohistochemistry (IHC)

Reconstructed skin and mouse skin specimens were stained using hematoxylin and eosin (H&E) according to standard procedures. IHC analysis was performed as previously described [cleaved caspase 3 (Asp175; 9664, Cell Signaling); Hsp70 (C92F3A-2, Enzo)] (Lamore and Wondrak, 2011). Detection of primary antibody was performed on a Discovery XT Automated Immunostainer (Ventana Medical Systems, Inc, Tucson, Arizona) using a biotinylated-streptavidin-HRP and DAB system. Hematoxylin counterstaining was also performed online. Images were captured using an Olympus BX50 camera.

Statistical analysis

The results are presented as means (± SD) of at least three independent experiments. Selected data sets were analyzed employing *one-way* analysis of variance (*ANOVA)* with Tukey's *post hoc* test using the Prism 4.0 software. In all bar graphs, means without a common letter differ ($p<0.05$).

Supplementary Material

Refer to Web version on PubMed Central for supplementary material.

ACKNOWLEDGEMENTS

Preliminary data from this research were part of an oral presentation at the Annual Meeting of the Society for Investigative Dermatology, May 8, 2014, Albuquerque, NM. Supported in part by grants from the National Institutes of Health [R03CA167580, R21CA166926, ES007091, ES006694].

Abbreviations

AhR	arylhydrocarbon receptor
FICZ	6-formylindolo[3,25*b*]carbazole
ICZ	6-formylindolo[3,2-*b*]carbazole
ROS	reactive oxygen species
UVA	ultraviolet A

REFERENCES

Agar NS, Halliday GM, Barnetson RS, et al. The basal layer in human squamous tumors harbors more UVA than UVB fingerprint mutations: A role for UVA in human skin carcinogenesis. PNAS. 2004; 101:4954–9. [PubMed: 15041750]

Agostinis P, Garmyn M, Van Laethem A. The Aryl hydrocarbon receptor: an illuminating effector of the UVB response. Sci STKE. 2007; 403:pe49. [PubMed: 17848686]

Andley UP, Clark BA. Generation of oxidants in the near-UV photooxidation of human lens alpha-crystallin. Invest Ophthalmol Vis Sci. 1989; 30:706–13. [PubMed: 2703311]

Baier J, Maisch T, Maier M, et al. Singlet oxygen generation by UVA light exposure of endogenous photosensitizers. Biophys J. 2006; 91:1452–9. [PubMed: 16751234]

Cadet J, Douki T, Ravanat JL, et al. Sensitized formation of oxidatively generated damage to cellular DNA by UVA radiation. Photochem Photobiol Sci. 2009; 8:903–11. [PubMed: 19582264]

Esser C, Bargen I, Weighardt H, et al. Functions of the aryl hydrocarbon receptor in the skin. Semin Immunopathol. 2013; 35:677–91. [PubMed: 23949496]

Fritsche E, Schafer C, Calles C, et al. Lightening up the UV response by identification of the arylhydrocarbon receptor as a cytoplasmatic target for ultraviolet B radiation. Proc Natl Acad Sci U S A. 2007; 104:8851–6. [PubMed: 17502624]

Gaitanis G, Magiatis P, Hantschke M, et al. The *Malassezia* Genus in Skin and Systemic Diseases. Clin Microbiol Rev. 2012; 25:106–41. [PubMed: 22232373]

Haarmann-Stemmann T, Abel J, Fritsche E, et al. The AhR-Nrf2 pathway in keratinocytes: on the road to chemoprevention? J Invest Dermatol. 2012; 132:7–9. [PubMed: 22158605]

Katiyar SK, Matsui MS, Mukhtar H. Ultraviolet-B exposure of human skin induces cytochromes P450 1A1 and 1B1. J Invest Dermatol. 2000; 114:328–33. [PubMed: 10651994]

Kennedy JC, Pottier RH. Endogenous protoporphyrin IX, a clinically useful photosensitizer for photodynamic therapy. J Photochem Photobiol B. 1992; 14:275–92. [PubMed: 1403373]

Kipp C, Young AR. The soluble eumelanin precursor 5,6-dihydroxyindole-2-carboxylic acid enhances oxidative damage in human keratinocyte DNA after UVA irradiation. Photochem Photobiol. 1999; 70:191–8. [PubMed: 10461458]

Lamore SD, Azimian S, Horn D, et al. The malondialdehyde-derived fluorophore DHP-lysine is a potent sensitizer of UVA-induced photooxidative stress in human skin cells. J Photochem Photobiol B. 2010a; 101:251–64. [PubMed: 20724175]

Lamore SD, Cabello CM, Wondrak GT. The topical antimicrobial zinc pyrithione is a heat shock response inducer that causes DNA damage and PARP-dependent energy crisis in human skin cells. Cell Stress Chaperones. 2010b; 15:309–22. [PubMed: 19809895]

Lamore SD, Qiao S, Horn D, et al. Proteomic identification of cathepsin B and nucleophosmin as novel UVA-targets in human skin fibroblasts. Photochem Photobiol. 2010c; 86:1307–17. [PubMed: 20946361]

Lamore SD, Wondrak GT. Zinc pyrithione impairs zinc homeostasis and upregulates stress response gene expression in reconstructed human epidermis. Biometals. 2011; 24:875–90. [PubMed: 21424779]

Luecke S, Backlund M, Jux B, et al. The aryl hydrocarbon receptor (AHR), a novel regulator of human melanogenesis. Pigment Cell Melanoma Res. 2010; 23:828–33. [PubMed: 20973933]

Magiatis P, Pappas P, Gaitanis G, et al. Malassezia yeasts produce a collection of exceptionally potent activators of the Ah (dioxin) receptor detected in diseased human skin. J Invest Dermatol. 2013; 133:2023–30. [PubMed: 23448877]

Marionnet C, Pierrard C, Lejeune F, et al. Different oxidative stress response in keratinocytes and fibroblasts of reconstructed skin exposed to non extreme daily-ultraviolet radiation. PLoS One. 2010; 5:e12059. [PubMed: 20706594]

Menon EL, Morrison H. Formation of singlet oxygen by urocanic acid by UVA irradiation and some consequences thereof. Photochem Photobiol. 2002; 75:565–9. [PubMed: 12081316]

Mukai M, Tischkau SA. Effects of tryptophan photoproducts in the circadian timing system: searching for a physiological role for aryl hydrocarbon receptor. Toxicol Sci. 2007; 95:172–81. [PubMed: 17020875]

Oberg M, Bergander L, Hakansson H, et al. Identification of the tryptophan photoproduct 6-formylindolo[3,2-b]carbazole, in cell culture medium, as a factor that controls the background aryl hydrocarbon receptor activity. Toxicol Sci. 2005; 85:935–43. [PubMed: 15788723]

Qiao S, Tao S, Rojo de la Vega M, et al. The antimalarial amodiaquine causes autophagic-lysosomal and proliferative blockade sensitizing human melanoma cells to starvation- and chemotherapy-induced cell death. Autophagy. 2013; 9:2087–102. [PubMed: 24113242]

Quintana FJ, Basso AS, Iglesias AH, et al. Control of T(reg) and T(H)17 cell differentiation by the aryl hydrocarbon receptor. Nature. 2008; 453:65–71. [PubMed: 18362915]

Rannug A, Fritsche E. The aryl hydrocarbon receptor and light. Biol Chem. 2006; 387:1149–57. [PubMed: 16972782]

Sato K, Taguchi H, Maeda T, et al. The primary cytotoxicity in ultraviolet-a-irradiated riboflavin solution is derived from hydrogen peroxide. J Invest Dermatol. 1995; 105:608–12. [PubMed: 7561167]

Scharffetter-Kochanek K, Wlaschek M, Brenneisen P, et al. UV-induced reactive oxygen species in photocarcinogenesis and photoaging. Biol Chem. 1997; 378:1247–57. [PubMed: 9426184]

Tigges J, Haarmann-Stemmann T, Vogel CF, et al. The new aryl hydrocarbon receptor antagonist E/Z-2-benzylindene-5,6-dimethoxy-3,3-dimethylindan-1-one protects against UVB-induced signal transduction. J Invest Dermatol. 2014; 134:556–9. [PubMed: 23995519]

Wei YD, Rannug U, Rannug A. UV-induced CYP1A1 gene expression in human cells is mediated by tryptophan. Chem Biol Interact. 1999; 118:127–40. [PubMed: 10359457]

Williams JD, Bermudez Y, Park SL, et al. Malondialdehyde-derived epitopes in human skin result from acute exposure to solar UV and occur in nonmelanoma skin cancer tissue. J Photochem Photobiol B. 2014; 132:56–65. [PubMed: 24584085]

Wincent E, Amini N, Luecke S, et al. The suggested physiologic aryl hydrocarbon receptor activator and cytochrome P4501 substrate 6-formylindolo[3,2-b]carbazole is present in humans. J Biol Chem. 2009; 284:2690–6. [PubMed: 19054769]

Wincent E, Bengtsson J, Mohammadi Bardbori A, et al. Inhibition of cytochrome P4501-dependent clearance of the endogenous agonist FICZ as a mechanism for activation of the aryl hydrocarbon receptor. Proc Natl Acad Sci U S A. 2012; 109:4479–84. [PubMed: 22392998]

Wondrak GT, Cabello CM, Villeneuve NF, et al. Cinnamoyl-based Nrf2-activators targeting human skin cell photo-oxidative stress. Free Radic Biol Med. 2008; 45:385–95. [PubMed: 18482591]

Wondrak GT, Jacobson EL, Jacobson MK. Photosensitization of DNA damage by glycated proteins. Photochem Photobiol Sci. 2002; 1:355–63. [PubMed: 12653475]

Wondrak GT, Jacobson MK, Jacobson EL. Endogenous UVA-photosensitizers: mediators of skin photodamage and novel targets for skin photoprotection. Photochem Photobiol Sci. 2006; 5:215–37. [PubMed: 16465308]

Wondrak GT, Roberts MJ, Cervantes-Laurean D, et al. Proteins of the Extracellular Matrix Are Sensitizers of Photo-oxidative Stress in Human Skin Cells. J Invest Dermatol. 2003; 121:578–86. [PubMed: 12925218]

Wondrak GT, Roberts MJ, Jacobson MK, et al. 3-hydroxypyridine chromophores are endogenous sensitizers of photooxidative stress in human skin cells. J Biol Chem. 2004; 279:30009–20. [PubMed: 15133022]

Wright A, Hawkins CL, Davies MJ. Photo-oxidation of cells generates long-lived intracellular protein peroxides. Free Radic Biol Med. 2003; 34:637–47. [PubMed: 12633741]

Zastrow L, Groth N, Klein F, et al. The missing link--light-induced (280-1,600 nm) free radical formation in human skin. Skin Pharmacol Physiol. 2009; 22:31–44. [PubMed: 19122479]

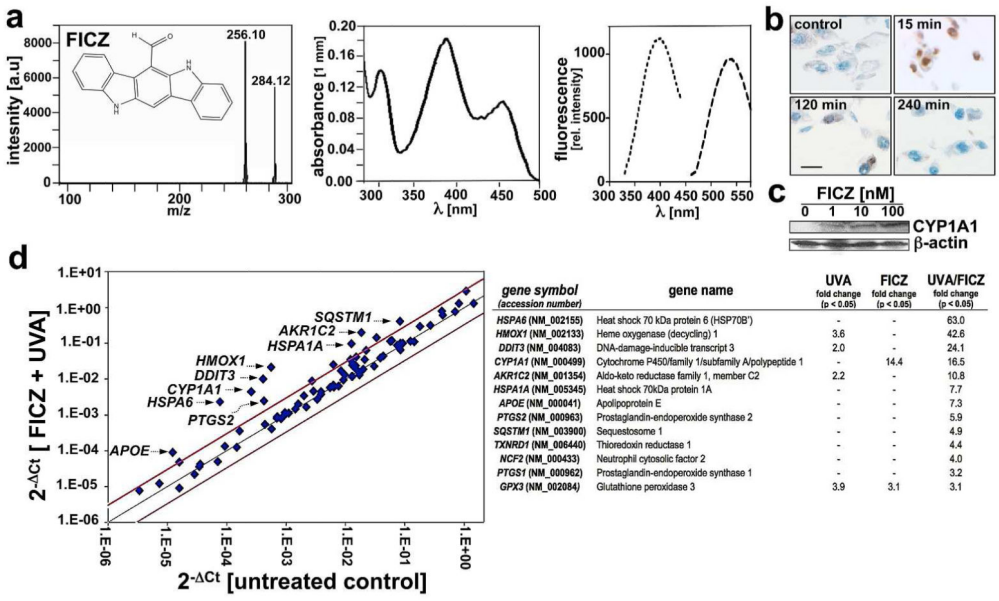

gene symbol (accession number)	gene name	UVA fold change (p < 0.05)	FICZ fold change (p < 0.05)	UVA/FICZ fold change (p < 0.05)
HSPA6 (NM_002155)	Heat shock 70 kDa protein 6 (HSP70B')	-	-	63.0
HMOX1 (NM_002133)	Heme oxygenase (decycling) 1	3.6	-	42.6
DDIT3 (NM_004083)	DNA-damage-inducible transcript 3	2.0	-	24.1
CYP1A1 (NM_000499)	Cytochrome P450/family 1/subfamily A/polypeptide 1	-	14.4	16.5
AKR1C2 (NM_001354)	Aldo-keto reductase family 1, member C2	2.2	-	10.8
HSPA1A (NM_005345)	Heat shock 70kDa protein 1A	-	-	7.7
APOE (NM_000041)	Apolipoprotein E	-	-	7.3
PTGS2 (NM_000963)	Prostaglandin-endoperoxide synthase 2	-	-	5.9
SQSTM1 (NM_003900)	Sequestosome 1	-	-	4.9
TXNRD1 (NM_006440)	Thioredoxin reductase 1	-	-	4.4
NCF2 (NM_000433)	Neutrophil cytosolic factor 2	-	-	4.0
PTGS1 (NM_000962)	Prostaglandin-endoperoxide synthase 1	-	-	3.2
GPX3 (NM_002084)	Glutathione peroxidase 3	3.9	3.1	3.1

Figure 1. The AhR agonist FICZ is a sensitizer of UVA-induced stress response gene expression in HaCaT keratinocytes

(**a**) left: electrospray MS-MS (positive ion mode); molecular ion (m/z 284); Δm 28 u: loss of carbonyl; middle: UV-VIS spectrum; right: fluorescence spectra [excitation spectrum (λem 530 nm); emission spectrum (λex 390 nm)]. (**b**) AhR nuclear translocation (FICZ: 100 nM; ≤ 240 min; scale bar 10 μ). (**c**) CYP1A1 Western blot analysis (16 h). (**d**) Oxidative Stress RT^2 Profiler™ PCR Expression Array analysis. After irradiation (UVA: 6.6 J/cm^2) in the presence or absence of FICZ (100 nM), cells were rinsed and then cultured in medium (6 h) followed by analysis; *left*: FICZ/UVA-induced gene expression (versus untreated), cut-off lines: threefold up- or down-regulation; *right*: Numerical expression changes (UVA only; FICZ only; FICZ/UVA versus untreated [n=3, mean ± SD; ($p<0.05$)].

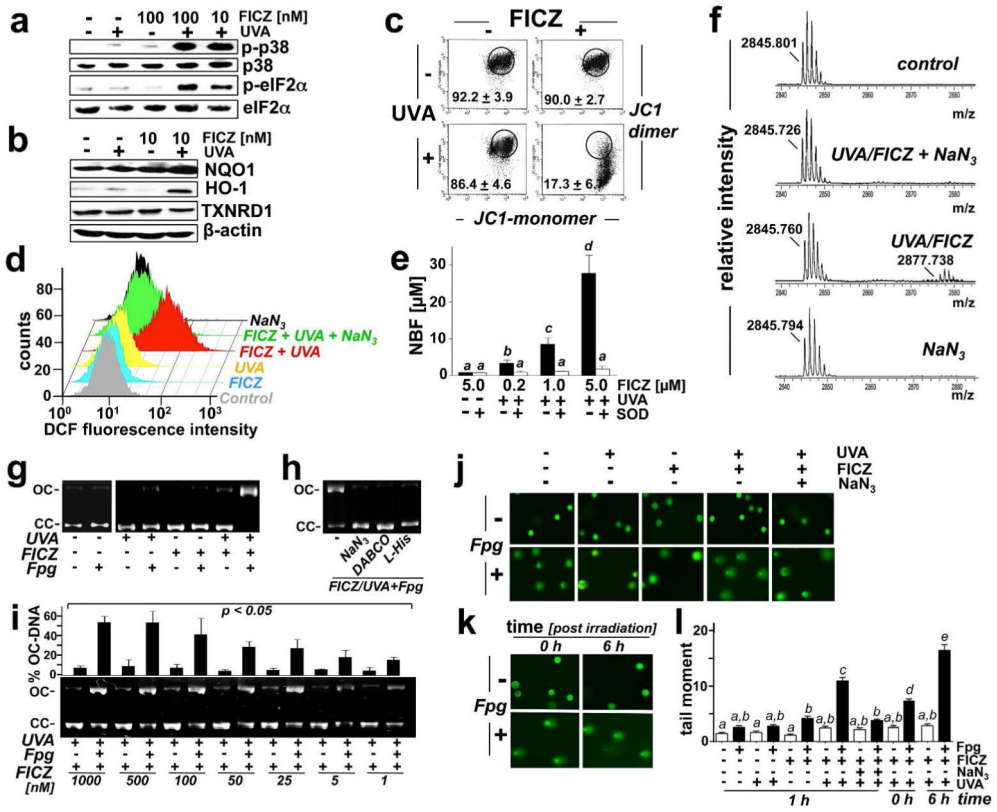

Figure 2. FICZ photodynamic activity causes oxidative stress and impairs genomic integrity

(**a**) Western blot analysis after UVA (6.6 J/cm^2) in the absence or presence of FICZ: phosphorylation of p38 and eIF2α (1 h after exposure). (**b**) Western blot analysis performed as in (a): NQO1, HO-1, TXNRD1 (6 h after exposure). (**c**) Mitochondrial transmembrane potential (Δψm) (10 nM FICZ; 6.6 J/cm^2 UVA; 1 h); numbers: percentage of cells inside the circle with intact Δψm (mean ± S.D., n=3). (**d**) Intracellular oxidative stress by flow cytometry of DCF fluorescence [UVA (3.3 J/cm^2); FICZ (20 nM); NaN_3 (10 mM); 1 h]. (**e**) UVA (3.3 J/cm^2)-driven superoxide production assessed by NBT reduction with (black) or without (white) SOD (3,000 u/ml). (**f**) MS analysis of peptide photooxidation. Monoisotopic mass peaks are indicated. (**f-l**) FICZ/UVA-induced ΦX174-plasmid cleavage enhanced by Fpg-digestion. (*OC*: open circular; *CC* closed circular; FICZ: 10 nM; UVA: 6.6 J/cm^2); (**h**) with inclusion of chemical antioxidants (10 mM, each); (**i**) dose response (UVA: 6.6 J/cm^2). (**j-l**) Fpg-enhanced Comet assay (FICZ: 100 nM; UVA: 6.6 J/cm^2; 20 mM NaN_3 (analysis post treatment: panel i: 1 h). (**l**) Tail moment analysis (n ≥ 100 per group; mean ± S.E.M).

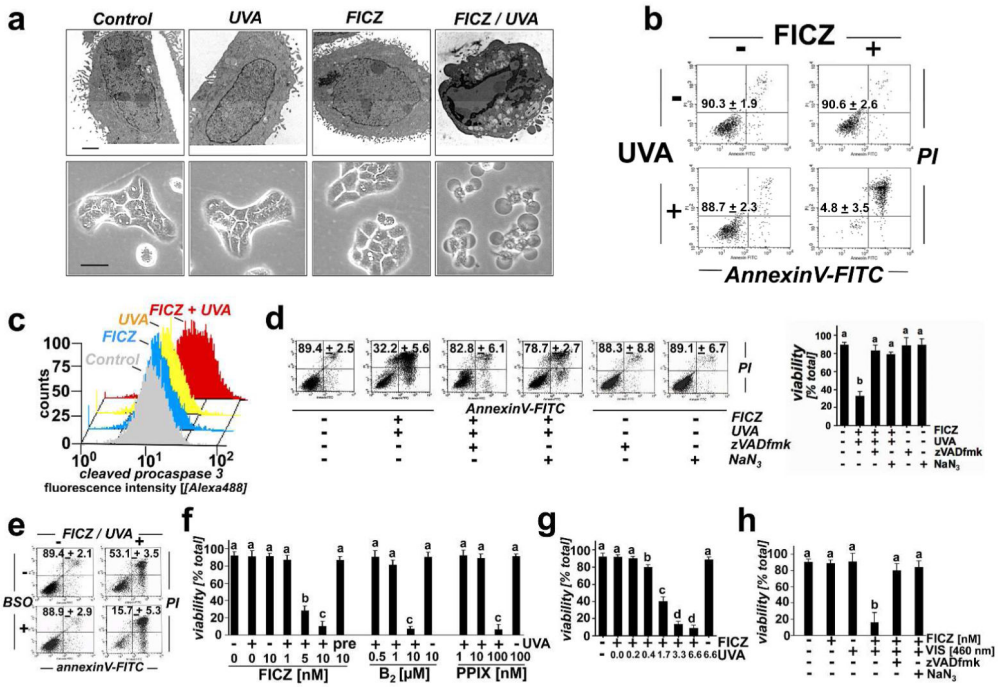

Figure 3. FICZ is a nanomolar sensitizer of UVA- and blue light-induced apoptosis

(**a**) HaCaT keratinocytes were exposed to the isolated or combined action of FICZ (100 nM) and UVA (6.6 J/cm^2) or remained untreated (control). Transmission electron (upper panels; 2,650 fold magnification; scale bar: 2 μ) or light microscopy (scale bar: 10 μ) after 6 h incubation in medium. (**b**) Flow cytometric analysis of annexinV-FITC/PI-stained cells (24 h after treatment as in panel a). Numbers indicate viable (AV$^-$/PI) in percent of total gated cells (mean ± S.D.; n = 3). (**c**) Flow cytometric detection of cleaved procaspase 3. (**d**) Cytoprotection against FICZ-induced cell death by zVADfmk (40 μM; 1 h pretreatment) or NaN_3 (10 mM; coincubation during UVA; FICZ: 20 nM; UVA: 1 J/cm^2). (**e**) Glutathione depletion-enhanced apoptosis (BSO: 1 mM, 24 h pretreatment; conditions as in panel d). (**f-h**) FICZ-induced apoptosis assessed as in Figure 3b. (**f**) FICZ dose response relationship (UVA: 6.6 J/cm^2). Photodynamic induction of cell death (UVA: 6.6 J/cm^2) using riboflavin (B_2) and protoporphyrin IX (PPIX) is also depicted. (**g**) UVA dose response relationship (FICZ: 100 nM). (**h**) Blue light (LED 460 nm; 2.5 J/cm^2)-induced apoptosis (FICZ: 100 nM; zVADfmk/NaN_3 as above; mean ± S.D., n ≥ 3).

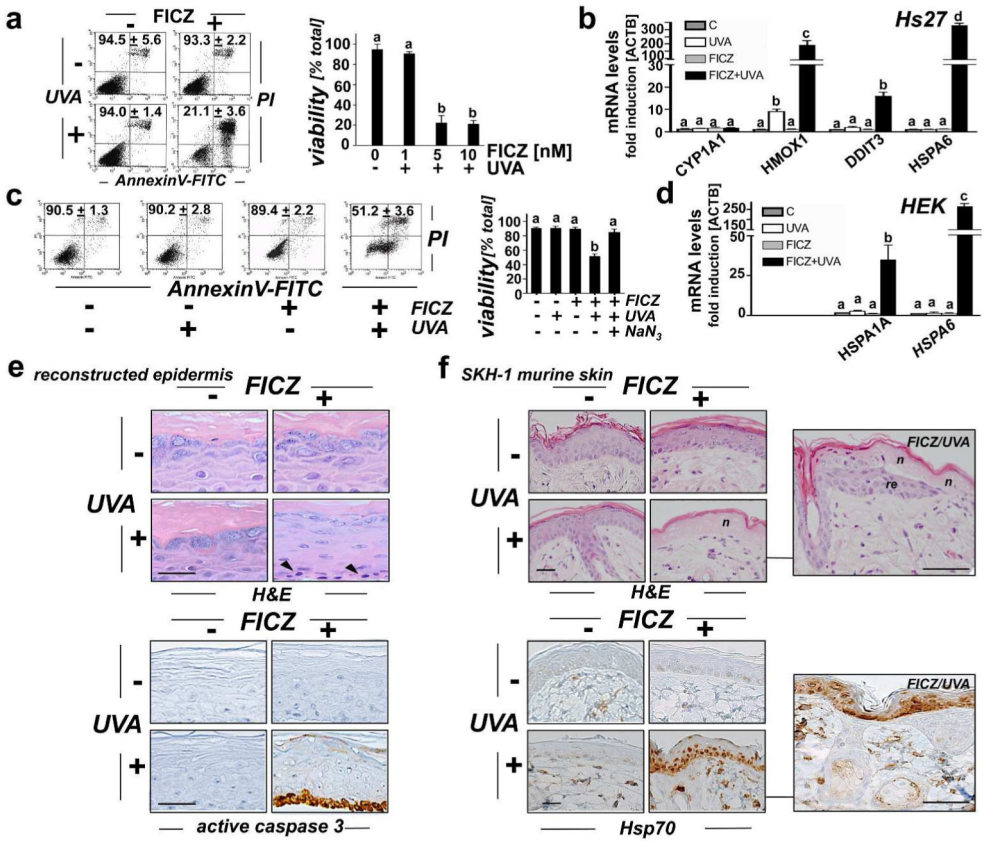

Figure 4. UVA-induced photodynamic activity of FICZ is observable in primary human epidermal keratinocytes, reconstructed epidermis, and mouse skin

(**a**)Human dermal Hs27 fibroblasts were exposed to the isolated or combined action of FICZ (100 nM) and UVA (6.6 J/cm^2) or remained untreated (control). After 24 h, viability was assessed as in Figure 3b; bar graph: FICZ dose response relationship of UVA-induced phototoxicity (UVA 6.6 J/cm^2). (**b**) Gene expression changes at the mRNA level after exposure to the isolated or combined action of FICZ (100 nM) and UVA [6.6 J/cm^2; 6 h after treatment; n=3, mean ± SD; ($p<0.05$)]. (**c**) Primary human epidermal keratinocytes (HEKs) exposed and analyzed as described in Figure 4a. (**d**) Gene expression changes in HEKs treated and analyzed as in Figure 4b. (**e)** Epidermal reconstruct (Epiderm™) specimens were cultured in growth medium supplemented with or without FICZ (100 nM; 6 h). After culture, UVA (6.6 J/cm^2) or mock-irradiation occurred. After 24 h, reconstructs were processed for IHC; arrowheads: localization of apoptotic basal keratinocytes (H&E: pycnotic/eosinophilic features, IHC: cleaved procaspase 3). (**f**) SKH-1 hairless mice (n=3 per treatment group) were exposed to the isolated or combined action of topical FICZ (1 mM) and UVA (6.6 J/cm^2) radiation. 48 h after treatment, H&E and IHC (Hsp70) analysis revealed photodynamic effects including epidermal necrosis (‘*n*’) and re-epithelialization (‘*re*’). Per treatment group, representative images taken from three repeat samples are displayed (scale bars = 25 μm; right insert, panel F: 50 μm).